EARTHQUAKE ENGINEERING AND STRUCTURAL DYNAMICS
Earthquake Engng. Struct. Dyn. **28**, 393–420 (1999)

REAL-TIME ON-LINE TEST FOR MDOF SYSTEMS

MASAYOSHI NAKASHIMA[1,*,†] AND NOBUAKI MASAOKA[2,‡]
[1] *Disaster Prevention Research Institute, Kyoto University, Gokasho, Uji, Kyoto 611-0011, Japan*
[2] *NTT Facilities, 3-4-1, Shibaura, Minato, Tokyo 108-023, Japan*

SUMMARY

This paper presents a test system for conducting on-line tests in a real time and a series of real-time on-line tests conducted to verify the effectiveness of the system. The proposed system is characterized by (1) use of a Digital Signal Processor (DSP) now readily available, (2) adoption of the C language to ensure easy programming, and (3) separation of response analysis and displacement signal generation to apply the system for tests with complex structures. To create displacement signals successively without being interrupted by the computation of equations of motion, extrapolation and interpolation procedures using present and past target displacements are developed. Base-isolated building models were chosen for the real-time on-line test. The effectiveness of the extrapolation and interpolation procedures was demonstrated through a series of real-time on-line tests applied to the models treated as SDOF structures. A five-storey base-isolated building model (treated as a six DOF structure) was tested for various ground motions, and it was verified that the system is able to simulate earthquake responses involving large displacements and large velocities. The number of DOFs that can be handled in the proposed system was investigated, and it was found that the system is capable of performing the test with reasonable accuracy for up to 10 DOF structures with a range of response frequency not greater than 3·0 Hz, or 12 DOF structures with a range of response frequency not greater than 2·0 Hz. Copyright © 1999 John Wiley & Sons, Ltd.

KEY WORDS: on-line test; real-time loading; DSP; MDOF system; base isolation

INTRODUCTION

The on-line computer controlled test (also referred to as the pseudo-dynamic test and simply called the on-line test in this paper) is an experimental technique for simulating the earthquake response of structures and structural components with respect to the time domain. In this test, the structural system is represented as a discrete spring–mass system, and is solved for its earthquake response using direct integration. Unlike conventional direct integration algorithms, in the on-line test the restoring forces of the system are not modelled but are directly measured

* Correspondence to: Masayoshi Nakashima, Disaster Prevention Research Institute, Kyoto University, Gokasho, Uji, Kyoto 611-0011, Japan. E-mail: nakashima@archi.kyoto-u.ac.jp
† Associate Professor
‡ Engineer

Contract/grant sponsor: Kajima Foundation

CCC 0098–8847/99/040393–28$17·50

Received 30 June 1998
Revised 12 October 1998

from a test conducted in parallel with the direct integration. One of the most significant advantages of the on-line test over the shaking table test is that the on-line test does not require dynamic loading although it is for simulating the earthquake response of the structure tested. This slow (quasi-static) loading makes larger scale testing possible because quasi-static loading actuators can be much larger in their load applying capacity than dynamic actuators if compared for the same hydraulic power. Slower loading also permits closer observation of the response behaviour of the structure. The essentials of the online test and previous applications are documented elsewhere (see for example References 1–6).

One of the critical prerequisites for conducting the on-line test is that the effect of the loading rate on the restoring force of the structure should be secondary because, in a real earthquake, the structure would be loaded dynamically. Lately, a variety of new types of structural components and devices have been introduced in structures, particularly in connection with their vibration control. These new devices include rubber bearings, viscous dampers, friction dampers, and sloshing dampers, many of which are very velocity dependent in their vibration characteristics. Unfortunately, the conventional on-line test based on quasi-static loading is not applicable for simulating the earthquake response of structures equipped with such devices.

This paper presents an on-line test system capable of applying on-line tests to structures whose restoring force characteristics are strongly dependent on velocity. In this system, the test structure is loaded dynamically in a real time; hence the system is hereinafter called the real-time on-line test system. The paper consists of two parts. In the first part, the architecture of the proposed system is detailed. First, similar systems developed previously are reviewed, and the proposed system is characterized in terms of its differences from and advantages over the previous systems. Second, major constituents of the system and their individual functions are detailed. Third, extrapolation, interpolation, and delay compensation procedures devised specifically for accurate displacement and velocity control are explicated. The second part presents a series of tests conducted to verify the effectiveness of the proposed system. The test structures are base-isolated building models. The substructuring technique[7,8] is employed in the test, and a base-isolation system comprising high damping rubber bearings is treated as the tested part, while the superstructure is treated analytically. First, the base-isolation system is modelled as an SDOF structure, and the performance of the proposed system is calibrated in terms of the effectiveness of the extrapolation, interpolation, and delay compensation procedures. Second, real-time on-line tests are carried out for a five-storey base-isolated building model, and the accuracy of the earthquake responses of the structure subjected to various ground motions is evaluated. Third, the number of DOFs that can be handled by the system is examined. Last, the capacities and limitations of the proposed system are appraised in terms of advantages and drawbacks relative to the shaking-table test.

REVIEW OF PREVIOUS REAL-TIME ON-LINE TEST SYSTEMS

As of today, two real-time on-line test systems are notable.[9,10] The very first real-time on-line test system was developed by Nakashima *et al.*[9] and applied to an SDOF system loaded by a single actuator. The basic procedures remained the same as those developed for conventional on-line testing, but a dynamic actuator replaced a quasi-static actuator to make the test structure loaded dynamically. A digital servo-mechanism was also devised and inserted between the computer (which solves the equation of motion) and the dynamic actuator in order to secure accurate

displacement and velocity control. This mechanism has the following tasks, namely: (1) to receive from the computer the target (computed) displacement, i.e. the displacement to be attained after an integration time interval (Δt), and the velocity required to reach this displacement; (2) to interpolate the target displacement linearly into a set of displacement signals for the interval of δt ($<\Delta t$) and (3) to send forward the signals successively with this interval to the actuator's servo-controller, while receiving the feedback displacement after every δt for feedback control. The system was devised with the electronic technologies of the late 1980s, and therefore the integration time interval (Δt) had to be relatively large (20 ms) and the displacement signal generated in the digital servo-mechanism was for a time interval (δt) of 2 ms. Because of these time constraints, the system was applied only to an SDOF system and could trace responses with primary frequencies of at most about 1·0 Hz.

Using more advanced electronic technologies in the 1990s, Horiuchi *et al.*[10] devised a special computing and controlling mechanism and proposed a new on-line system capable of performing real-time on-line tests The mechanism, designated as a super real-time controller, can complete one cycle of computation/control in under 0·5 ms. To secure such fast execution, parallel computing techniques are adopted, and a special computation language was invented.[11] The system was applied successfully to real-time on-line tests of a few model structures treated as up to four DOF systems,[12–14] with one DOF tested and the others treated numerically using the substructuring technique.

The system developed by Horiuchi *et al.*[10] is very sophisticated, but following problems may hinder the wide application of the real-time on-line test. First, the system requires a special device and a special programming language. Considering the nature of structural testing, the program for solving the equations of motion must vary from test to test in accordance with the type of structure examined, and therefore inflexibility of programming (caused by requiring the use of an esoteric language) is not necessarily desirable. Second, the equations of motion are solved with an integration time interval of 0·5 ms in order to send the target (computed) displacement to the actuator's servo-controller after every 0·5 ms, the time required for one cycle of operation. In most earthquake response analyses using direct integration, however, an integration time interval in a range of 10 ms is sufficient, which means that the interval of 0·5 ms is too small from the viewpoint of response analysis. If a longer time is allowed for solving the equations of motion, a slower computer can be used, or the system can be applied to more complex structures involving many DOFs (requiring a longer computation time). To resolve these problems, the system proposed in this study has the following characteristics: (1) a widely available digital signal processor (DSP) is used for solving the equations of motion; (2) a popular programming language C is used to enable flexible programming for the solution of the equations of motion and (3) the task of creating the target displacement (by solving the equations of motion) at an integration time interval (Δt) and the task of creating displacement signals (to be sent to the servo-controller) at a smaller time interval (δt) are separated so that the time requirement for solving the equations of motion can be less stringent. The idea of separating the two tasks follows what was adopted in the very first application of the real-time on-line test.[9]

SYSTEM

The outline of the proposed system is shown in Figure 1. The system consists of an electro servo-controlled actuator with hydraulic power, a digital servo-controller that supervises the

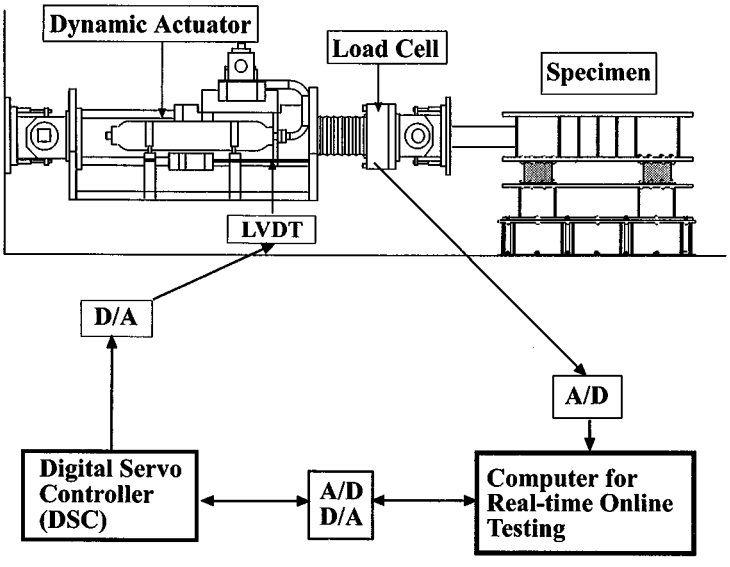

Figure 1. Outline of proposed real-time on-line test system

actuator motion, a test specimen (rubber bearings of a base-isolated building in this study), a displacement transducer to measure the displacement of the actuator, a load cell to measure the reactional force of the specimen, and a newly devised computer, called the computer for real-time on-line testing, that creates the target displacements and displacement signals and send them to the digital servo-controller. The system developed thus far is for a single dynamic actuator, but use of the substructuring technique is contemplated, and therefore the equations of motion to be solved are for multiple DOFs.

Dynamic actuator and digital servo-controller

The dynamic actuator, equipped with an electro servo-valve having a flow capacity of 1470 l/min, can produce ± 750 kN in force, ± 250 mm in displacement, and 600 mm/s in velocity. The displacement and force of the actuator are measured by an LVDT with a stroke of ± 300 mm and a load cell of $\pm 1{\cdot}0$ MN in capacity. The actuator motion is controlled by a digital servo-controller whose major tasks are executed by a DSP having a central memory of 512 kbytes, a supplementary memory of 16 Mbytes, and an execution speed of 61 ns. The DSP is also equipped with 16 A/D and 8 D/A channels, both having a resolution of 16 bits and a sampling speed of 5 μs. The major tasks of the controller are: (1) to receive the target command value, for example, the target displacement, and the time required to attain the value, both in digital form and (2) to keep generating command signals and sending them to the actuator after D/A conversion, while also receiving feedback signals to ensure accurate control. This digital servo-controller is of a standard type, now widely used in controlling hydraulic servo-controlled actuators.

Computer for real-time on-line test

This computer is the key component in carrying out the real-time on-line test, and the major tasks are executed by a DSP whose specifications are identical with the DSP used for the digital servo-controller. The computer has two tasks: (1) the task of creating the target displacement by solving the equations of motion with an integration time interval of Δt, called 'Response Analysis Task', and (2) the task of creating successive displacement signals with a smaller time interval of δt (to ensure smooth actuator motion) and sending the signals to the digital servo-controller, called 'Signal Generation Task'. These two tasks are programmed in the C language and developed separately as independent procedures. These two procedures are essentially encapsulated with each other, so that variables that the two tasks have to share are limited only to the integration time interval (Δt), the target displacement at an interval of Δt, and the measured displacement and force also at an interval of Δt. The use of the C language and the separation and minimum interchange of the two tasks ensure flexible programming, particularly for the solution of the equations of motion.

To ensure continuous real-time loading, the computer for the real-time on-line test has to keep sending displacement signals without any interruption to the digital servo-controller. On the other hand, the next target displacement is not ready at the instant when loading in the current integration time step is completed. To overcome this problem, 'Signal Generation Task' is programmed so that it continues to send displacement signals with the interval of δt even if the target displacement is not given, and the signals are generated by the extrapolation of previous displacements [Figure 2(a)]. In the meantime, 'Response Analysis Task' executes the program for obtaining the next target displacement. Once the 'Response Analysis Task' is completed and the target displacement is made available, 'Signal Generation Task' stops extrapolation and starts performing interpolation, trying to shoot the now obtained target displacement [Figure 2(b)]. This combined extrapolation and interpolation procedure will be explicated in the next section. In the proposed system, the integration time interval (Δt) is set at 10 ms, which is deemed small enough to ensure accurate response analysis of most structures, and the time interval (δt) for creating and sending displacement signals set at 1 ms, which was determined in reference to the DSP capacity. A schematic view of this whole operation is shown in Figure 3.

In the execution of the program, δt (1 ms) forms one cycle of operation (Figure 4). 'Signal Generation Task' (developing the displacement signal after 1 ms) is executed first (taking about

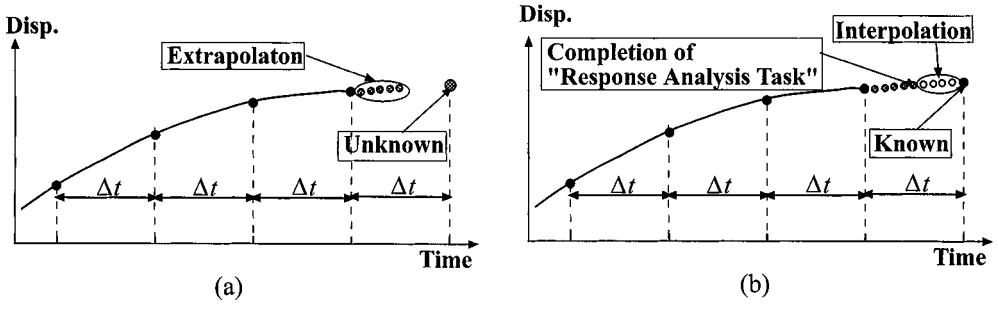

Figure 2. Extrapolation and interpolation procedures to assure real-time loading: (a) extrapolation; (b) interpolation

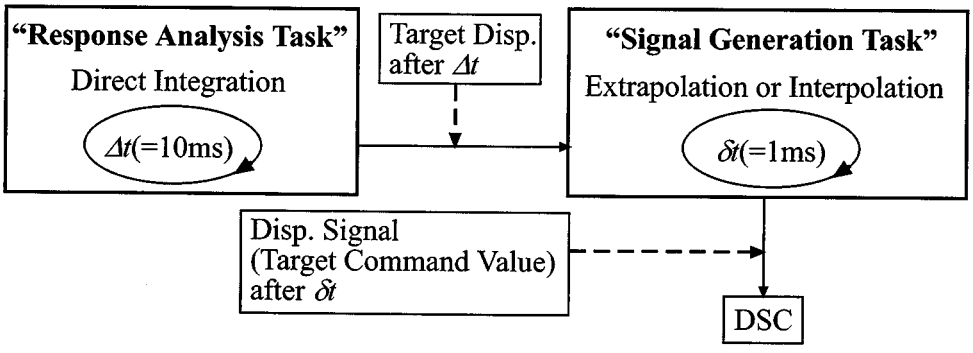

Figure 3. Separation of 'Response Analysis Task' and 'Signal Generation Task'

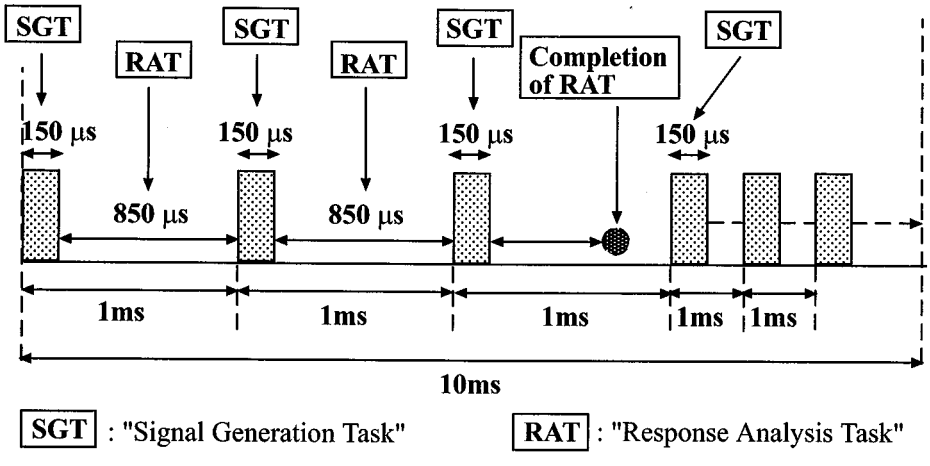

Figure 4. Execution sequence of 'Response Analysis Task' and 'Signal Generation Task'

150 μs, which was confirmed from a series of trial tests), and the rest of the time [about 850 (1000 − 150) ms] is spent to execute 'Response Analysis Task' [computing the target displacement after 10 ms ($=\Delta t$)]. If 'Response Analysis Task' is not completed and the target displacement is not yet obtained after 1 ms, 'Response Analysis Task' is paused, switched to 'Signal Generation Task' for obtaining the next displacement signal (by extrapolation), and switched again to 'Response Analysis Task' to resume the computation. This operation is repeated until 'Response Analysis Task' is completed and the target displacement is obtained, and then for the rest of the time only 'Signal Generation Task' is carried out (by interpolation). How many cycles of extrapolation are needed depends on the size of the program for solving the equations of motion, and the more DOFs are to be solved, the more cycles of extrapolation are required.

EXTRAPOLATION AND INTERPOLATION PROCEDURES

Extrapolation procedure

A very natural way to extrapolate the displacement is to utilize the displacements obtained at immediate past integration time steps. In this study, extrapolation using a Langangean polynomial is adopted. The higher-order polynomial is used, the better accuracy is normally obtained, but this requires more time for calculating the extrapolated displacement and more memory for storing the previous data, and therefore a trade-off between accuracy and computation time is required. The jth extrapolated displacement (x'_j) is expressed as

$$x'_j = \sum_{i=0}^{n} a'_{ij} x_i \tag{1}$$

where x_0 is the displacement most recently obtained, x_1 the target displacement one integration time step before, etc. [Figure 5(a)], a'_{ij} the coefficient associated with x_i, and n the order of the polynomial. For example, the coefficients for the third-order polynomial are as follows.

Third-order polynomial:

$$a'_{0j} = \frac{1}{6}\left(\frac{j\delta t}{\Delta t}+1\right)\left(\frac{j\delta t}{\Delta t}+2\right)\left(\frac{j\delta t}{\Delta t}+3\right), \qquad a'_{1j} = -\frac{1}{2}\frac{j\delta t}{\Delta t}\left(\frac{j\delta t}{\Delta t}+2\right)\left(\frac{j\delta t}{\Delta t}+3\right)$$

$$a'_{2j} = \frac{1}{2}\frac{j\delta t}{\Delta t}\left(\frac{j\delta t}{\Delta t}+1\right)\left(\frac{j\delta t}{\Delta t}+3\right), \qquad a'_{3j} = -\frac{1}{6}\frac{j\delta t}{\Delta t}\left(\frac{j\delta t}{\Delta t}+1\right)\left(\frac{j\delta t}{\Delta t}+2\right) \tag{2}$$

The accuracy of extrapolation can be evaluated as follows. Considering that structures vibrate in a sinusoidal fashion in earthquake responses, let us suppose that the structure vibrates sinusoidally with an amplitude A and a circular frequency ω as

$$x = A \sin \omega t \tag{3}$$

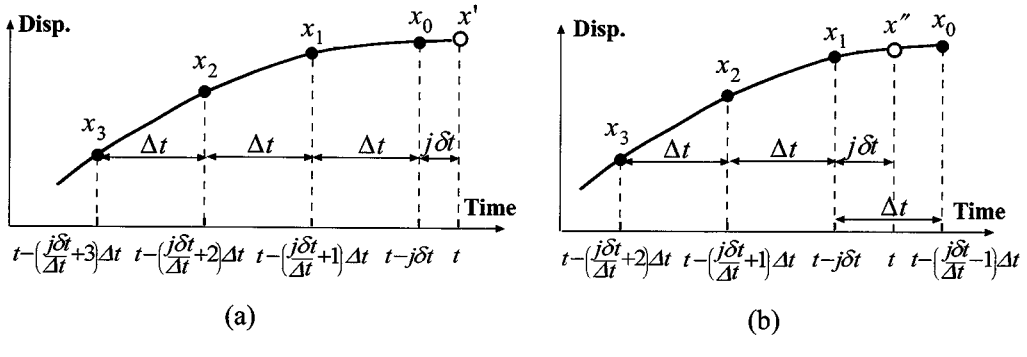

Figure 5. Third-order extrapolation and interpolation procedures: (a) extrapolation using previously obtained displacements; (b) interpolation using target and previously obtained displacements

Then, the previous displacements used for extrapolation for predicting the displacement at time t are expressed as

$$x_i = A \sin \omega \left\{ t - \left(\frac{j\delta t}{\Delta t} + i \right) \Delta t \right\} \tag{4}$$

Inserting equation (4) into equation (1), the extrapolated displacement is expressed as

$$\begin{aligned} x'_j &= \sum_{i=0}^{n} a'_{ij} A \sin \omega \left\{ t - \left(\frac{j\delta t}{\Delta t} + i \right) \Delta t \right\} = A \sum_{i=0}^{n} a'_{ij} \left\{ \sin \omega t \cos \omega \left(\frac{j\delta t}{\Delta t} + i \right) \Delta t \right. \\ &\quad \left. - \cos \omega t \sin \omega \left(\frac{j\delta t}{\Delta t} + i \right) \Delta t \right\} \\ &= A \sqrt{C'^2_j + S'^2_j} \sin(\omega t + \theta'_j) \end{aligned} \tag{5}$$

in which

$$C'_j = \sum_{i=0}^{n} a'_{ij} \cos \omega \left(\frac{j\delta t}{\Delta t} + i \right) \Delta t, \qquad S'_j = - \sum_{i=0}^{n} a'_{ij} \sin \omega \left(\frac{j\delta t}{\Delta t} + i \right) \Delta t, \; \theta'_j = \tan^{-1} \frac{S'_j}{C'_j} \tag{6}$$

Equation (5) indicates that the difference between the extrapolated and true displacements is characterized by an amplitude change of $\sqrt{C'^2_j + S'^2_j}$ and by a phase-lag of θ'_j. Figure 6 shows these characteristics obtained from extrapolations of the first-, second-, third-, and fourth-order polynomials with respect to the number of extrapolations (j) and the normalized integration time interval ($\omega \Delta t$). Obvious findings obtained from Figure 6 are: the extrapolated displacement is more distorted for (1) a larger number of extrapolations (j), (2) a larger integration time interval ($\omega \Delta t$) and (3) a lower-order polynomial (particularly when $\omega \Delta t$ is small). The integration time interval (Δt) should be small enough to ensure stability and accuracy of the direct integration for solving the equations of motion. For example, with ω as the natural frequency of the structure, $\omega \Delta t$ should be smaller than 2·0 to maintain solution stability in the central difference method, the one conventionally used in the on-line test, and $\omega \Delta t < 0{\cdot}3$–$0{\cdot}4$ is chosen in many cases for achieving accurate responses. From Figure 6, for smaller values of $\omega \Delta t$ (say, $\omega \Delta t < 0{\cdot}5$), the third- and fourth-order polynomials are about the same in accuracy and significantly better than the first- and second-order polynomials. For this reason and also for the reason of maintaining good accuracy in velocity, which will be described later, the third-order polynomial was adopted for the extrapolation procedure.

Interpolation procedure

If a polynomial function is used for interpolation, a formulation similar to that obtained for extrapolation can be derived. The jth interpolated displacement (x''_j) is expressed as

$$x''_j = \sum_{i=0}^{n} a''_{ij} x_i \tag{7}$$

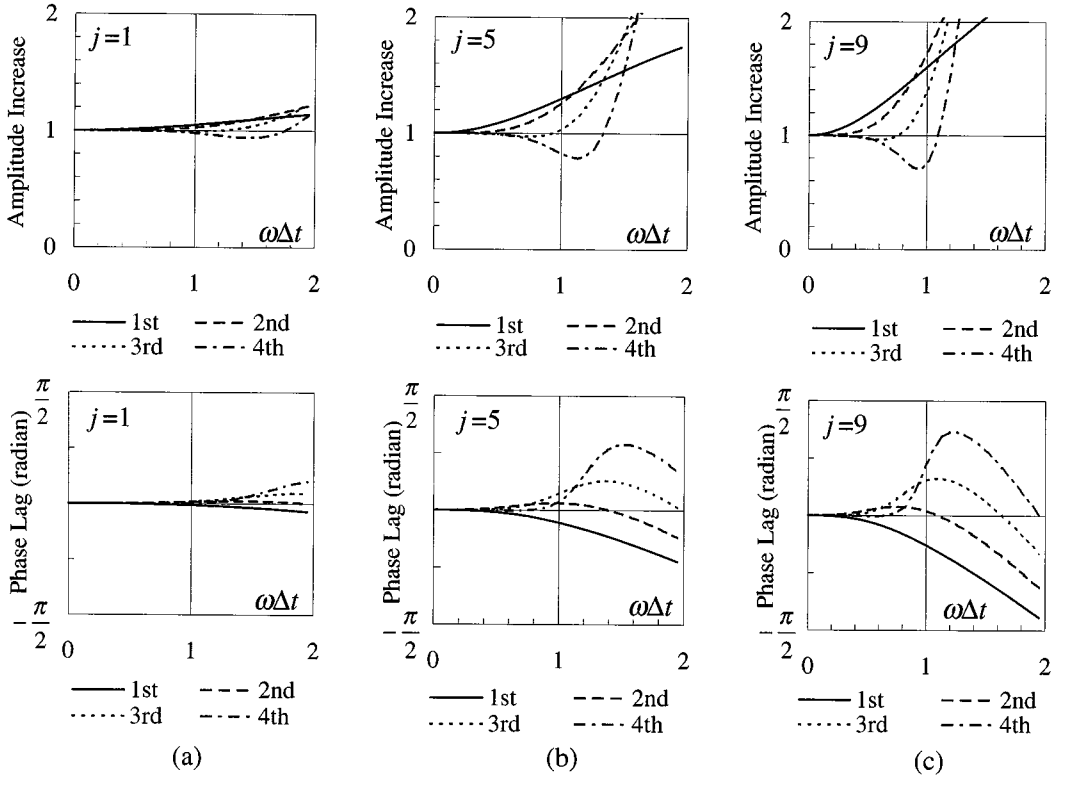

Figure 6. Accuracy of extrapolation in terms of amplitude change and phase lag: (a) $j = 1$; (b) $j = 5$; (c) $j = 9$

where x_0 is the next target displacement, x_1 the target displacement one integration time step before, etc. [Figure 5(b)], and a''_{ij} the coefficient associated with x_i. For example, the coefficients for the third-order polynomial are as follows.

Third-order polynomial:

$$a''_{0j} = \frac{1}{6}\frac{j\delta t}{\Delta t}\left(\frac{j\delta t}{\Delta t}+1\right)\left(\frac{j\delta t}{\Delta t}+2\right), \qquad a''_{1j} = -\frac{1}{2}\left(\frac{j\delta t}{\Delta t}-1\right)\left(\frac{j\delta t}{\Delta t}+1\right)\left(\frac{j\delta t}{\Delta t}+2\right)$$

$$a''_{2j} = \frac{1}{2}\left(\frac{j\delta t}{\Delta t}-1\right)\frac{j\delta t}{\Delta t}\left(\frac{j\delta t}{\Delta t}+2\right), \qquad a''_{3j} = -\frac{1}{6}\left(\frac{j\delta t}{\Delta t}-1\right)\frac{j\delta t}{\Delta t}\left(\frac{j\delta t}{\Delta t}+1\right) \tag{8}$$

With the assumption that the system vibrates sinusoidally as shown in equation (3), the displacements used for interpolation for predicting the displacement at time t are expressed as

$$x_i = A \sin\omega\left\{t - \left(\frac{j\delta t}{\Delta t} - 1 + i\right)\Delta t\right\} \tag{9}$$

Inserting equation (9) into equation (7), the interpolated displacement is expressed as

$$x''_j = A(C''_j \sin \omega t + S''_j \cos \omega t) = A\sqrt{C''^2_j + S''^2_j}\, \sin(\omega t + \theta''_j) \tag{10}$$

where

$$C''_j = \sum_{i=0}^{n} a''_{ij} \cos \omega \left(\frac{j\delta t}{\Delta t} - 1 + i \right) \Delta t, \qquad S''_j = -\sum_{i=0}^{n} a''_{ij} \sin \omega \left(\frac{j\delta t}{\Delta t} - 1 + i \right) \Delta t, \; \theta''_j = \tan^{-1} \frac{S''_j}{C''_j} \tag{11}$$

Equation (10) indicates that the difference between the interpolated and true displacements is characterized by an amplitude change of $\sqrt{C''^2_j + S''^2_j}$ and by a phase-lag of θ''_j. These characteristics, shown in Figure 7, indicate that interpolation is more accurate than extrapolation (Figure 6) if compared for the same j and $\omega\Delta t$. Furthermore, the error is very small regardless of $\omega\Delta t$ when $j = 9$ [the interpolated displacement is close to the target displacement: x_0 in Figure 5(b)] or $j = 1$ [the interpolated displacement is close to the target displacement one integration time interval before: x_1 in Figure 5(b)] and is largest in between ($j = 5$). Because the third-order polynomial was adopted for the extrapolation procedure, the same order polynomial was used for the interpolation procedure for the sake of consistency.

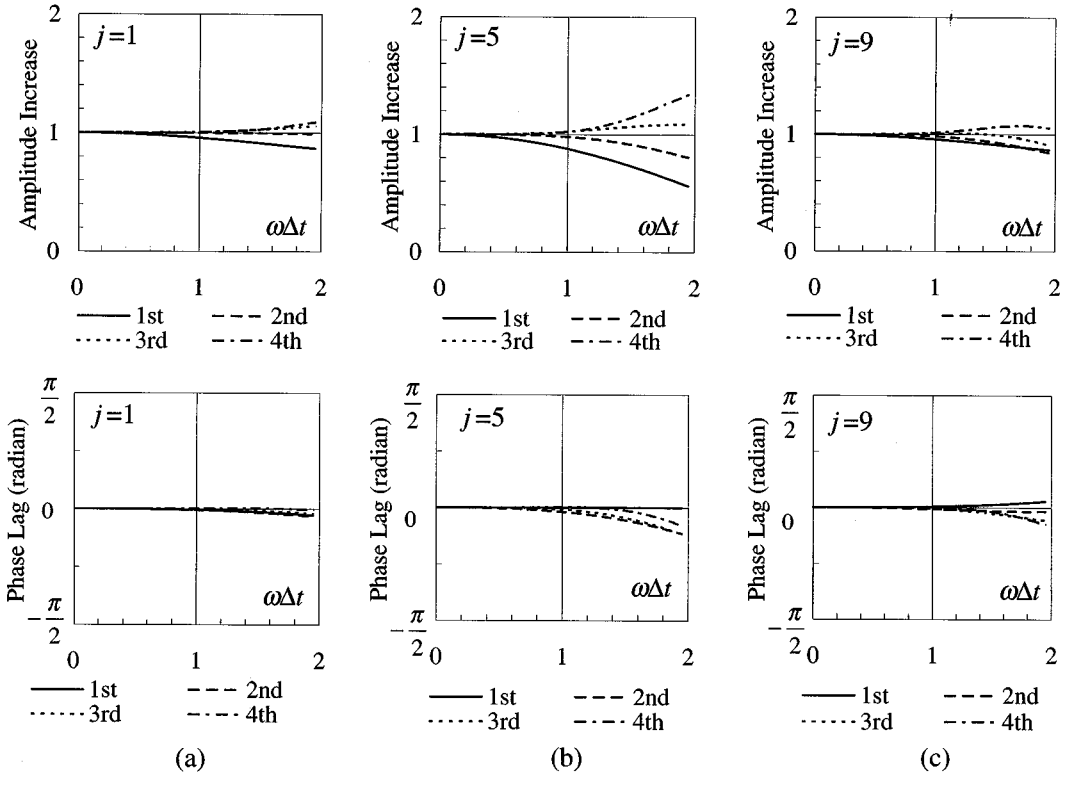

Figure 7. Accuracy of interpolation in terms of amplitude change and phase lag: (a) $j = 1$; (b) $j = 5$; (c) $j = 9$

Accuracy in velocity

In the proposed system, accurate velocity control is also very important. The largest concern is a sudden velocity change that may appear in the interval when the creation of the displacement signal switches from extrapolation to interpolation (Figure 8). The following numerical example provides a view of the velocity in the switching interval. A sinusoidal wave with an amplitude of 1 mm and a frequency of 1·0 Hz was considered and discretized with a time interval of 8 ms (representing one integration time step: Δt, with $\omega\Delta t$ nearly equal to 0·5). The number of extrapolations was assumed to be 5 ($j = 5$), meaning that the first five displacement signals [provided after every 1 ms (δt)] were generated by extrapolation, and the rest by interpolation. The difference between the sixth (the first interpolated) displacement signal and the fifth (last extrapolated) displacement signal, divided by δt, was taken as the velocity in the switching interval. Figure 9 shows this velocity obtained successively for every 8 ms (Δt), together with the true velocity, indicating that the velocity in the switching interval is more accurate for higher-order polynomials. It is also notable that in the first- and second-order polynomials the velocity phase is advanced, whereas in the third- and fourth-order polynomials the phase is delayed. For example, in reference to Figure 9(a), the true velocity is positive but the first- and second-order

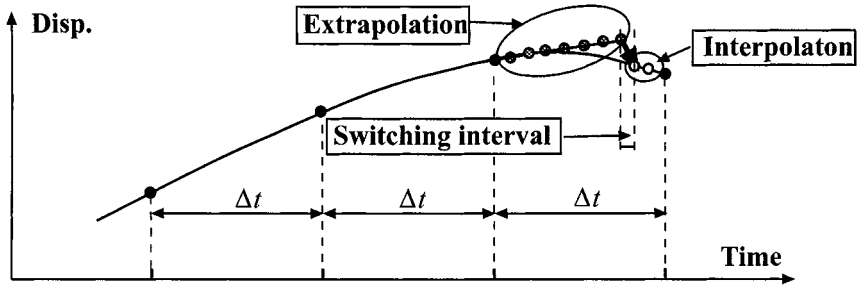

Figure 8. Velocity change in interval where extrapolation switches to interpolation

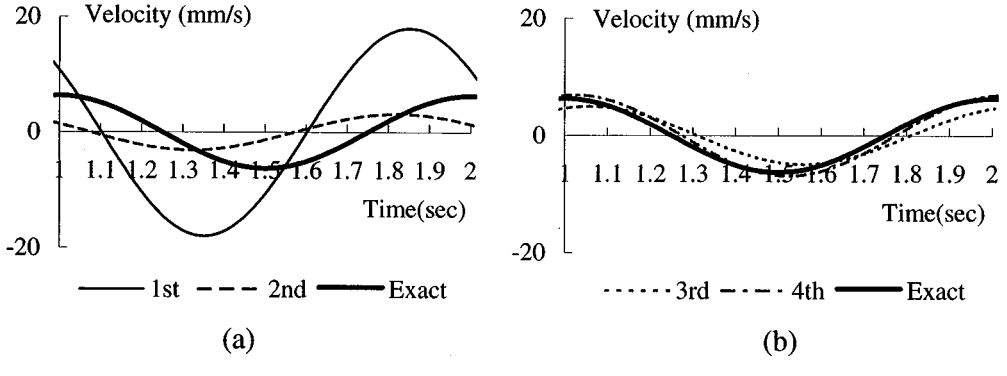

Figure 9. Velocity attained in switching interval ($\omega\Delta t = 0{\cdot}5, j = 5$); (a) first- and second-order polynomials; (b) third- and fourth-order polynomials

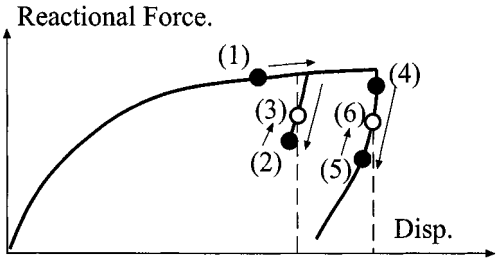

Figure 10. Effect of unloading and reloading caused by negative velocity in switching interval

polynomials give negative velocities between 1·1 and 1·25 s. If we consider the non-linear hysteresis curve shown in Figure 10, the displacement path (created after every 1 ms during the time interval of 8 ms) is as follows: (1) loading in the positive direction during extrapolation (because the true velocity is positive), (2) then unloading in the switching interval (because of the negative velocity as a result of switching from extrapolation to interpolation) and (3) loading again to the target displacement during interpolation. That is, overshooting and unloading is involved when the structure's deformation is yet to increase. It should be noted that such behaviour occurs when the true velocity approaches zero [Figure 9(a)], i.e., in the vicinity of the peak displacement. On the other hand, in reference to Figure 9(b), the true velocity becomes negative but the third- and fourth-order polynomials still give positive velocities in the switching interval between 1·25 and 1·3 s. For the non-linear hysteresis curve shown in Figure 10, the displacement path during the integration time interval of 8 ms is: (4) unloading after the peak displacement by extrapolation (because the true velocity is negative), (5) then reloading in the switching interval (because of the positive velocity in that interval) and (6) unloading again to the target displacement by interpolation. That is, partial reloading is involved during the time interval of 8 ms (Δt). Note that such reloading occurs at the beginning of unloading.

The velocity in the switching interval can be estimated in the following manner. Let us suppose that the system vibrates sinusoidally as shown in equation (3). The displacement (x'_j) at time t (after the jth extrapolation) is given by equation (5). In reference to equation (10), the displacement ($x''_{(j+1)}$) at time ($t + \delta t$) is given as

$$x''_{(j+1)} = A\{C''_{(j+1)} \sin \omega(t + \delta t) + S''_{(j+1)} \cos \omega(t + \delta t)\} \tag{12}$$

where

$$C''_{(j+1)} = \sum_{i=0}^{n} a''_{i(j+1)} \cos \omega \left\{ \frac{(j+1)\,\delta t}{\Delta t} - 1 + i \right\} \Delta t,$$

$$S''_{(j+1)} = -\sum_{i=0}^{n} a''_{i(j+1)} \sin \omega \left\{ \frac{(j+1)\,\delta t}{\Delta t} - 1 + i \right\} \Delta t \tag{13}$$

The velocity in the switching interval is

$$v'_j = \frac{x''_{(j+1)} - x'_j}{\delta t} = \frac{A}{\delta t} \sqrt{\tilde{C}_j^2 + \tilde{S}_j^2} \cos(\omega t - \tilde{\theta}_j) \tag{14}$$

where

$$\tilde{C}_j = C''_{(j+1)} \cos \omega\delta t - C'_j - S''_{(j+1)} \sin \omega\delta t, \qquad \tilde{S}_j = C''_{(j+1)} \sin \omega\delta t - S'_j + S''_{(j+1)} \cos \omega\delta t,$$

$$\tilde{\theta}_j = \tan^{-1} \frac{\tilde{C}_j}{\tilde{S}_j} \tag{15}$$

On the other hand, the true velocity is given by the first differentiation of equation (3):

$$v = A\omega \cos \omega t \tag{16}$$

Comparison between equations (14) and (16) shows that the velocity in the switching interval is characterized by the amplitude change of $\sqrt{\tilde{C}_j^2 + \tilde{S}_j^2}/\delta t$ and a phase lag of $\tilde{\theta}_j$. Figure 11 shows these changes for $j = 1$ (one cycle of extrapolation followed by interpolation) and $j = 5$ (five cycles of extrapolation followed by interpolation), indicating that the third- and fourth-order polynomials are significantly more accurate than the first- and second-order polynomials, and that the phase is advanced for the first- and second-order polynomials (see the negative sign before $\tilde{\theta}_j$ in equation (14)) and delayed for the third- and fourth-order polynomials. As illustrated in Figure 10, the velocity-phase advancement causes unloading in the switching interval when the structure is to be loaded toward the peak displacement, while the velocity-phase delay causes

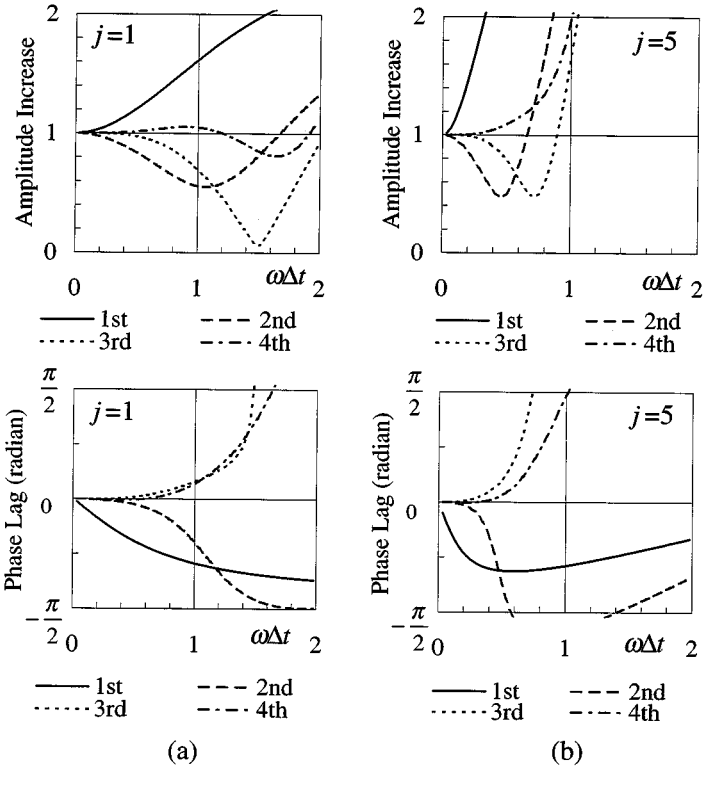

Figure 11. Accuracy of velocity in switching interval in terms of amplitude change and phase lag: (a) $j = 1$; (b) $j = 5$

reloading in the switching interval when the structure starts unloaded. Because most structures behave almost elastically in the initial unloading range, phase delay is much more acceptable than phase advancement: another strong reason that the third-order polynomial was adopted for the extrapolation and interpolation procedures.

ACTUATOR DELAY AND DELAY COMPENSATION

Actuator motion is delayed with respect to the commanded motion because of various flexibilities and inelasticities of the actuator–controller–specimen system. Such a delay causes little harm if the displacement command is specified *a priori* such as when the test structure is subjected to repeated sinusoidal motion, but the delay is very critical and tends to significantly aggravate the response in the on-line test. When the delay is present, the on-line test system detects the counterclockwise hysteresis loops erroneously, and these loops add energy into the system, causing divergent responses.[12,13,15] In the proposed system the delay compensation procedure developed by Horiuchi *et al.*[13] was adopted to avoid such erroneous responses. Let us suppose an instant when the test is completed up to time $(t - \delta t)$, the displacement signal for time t is calculated (either by extrapolation or interpolation) in 'Signal Generation Task', and the signal is ready to be sent to the digital servo-controller. Before sending this signal, the displacement signal at time $(t + \bar{\delta}t)$ is predicted, with $\bar{\delta}t$ as the actuator's delay time. Polynomial extrapolation is carried out for the prediction using the displacement signals at times t, $(t - \bar{\delta}t)$, $(t - 2\bar{\delta}t)$, etc. (Figure 12), and this predicted signal $(\bar{x})$ is sent to the digital servo-controller instead of the displacement signal originally calculated (x_0). Because of the actuator delay of $\bar{\delta}t$, the displacement achieved at time t should be very close to the original displacement. The third-order polynomial was used for predicting the displacement signal. Before the real-time on-line test, the initial delay time $(\bar{\delta}t)$ was estimated from preliminary dynamic loading tests subjected to forced sinusoidal displacements. The delay time was kept updated after every half cycle (meaning from a zero-crossing displacement to the next zero-crossing displacement) during the real-time on-line test. Full details of this delay compensation procedure are presented elsewhere.[13,14]

TEST SETUP AND TEST SPECIMEN

The proposed test system was used to simulate earthquake responses of base-isolated building models. The substructuring technique was employed as shown in Figure 13: the base-isolation

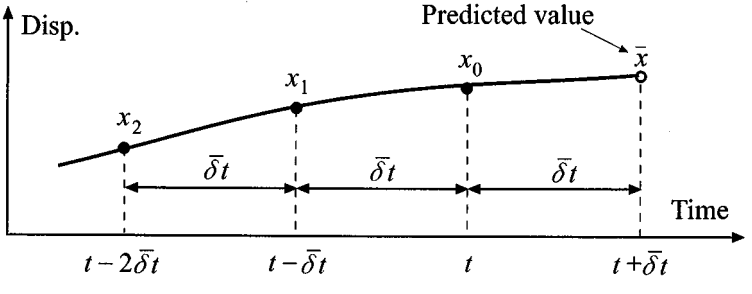

Figure 12. Actuator delay compensation procedure

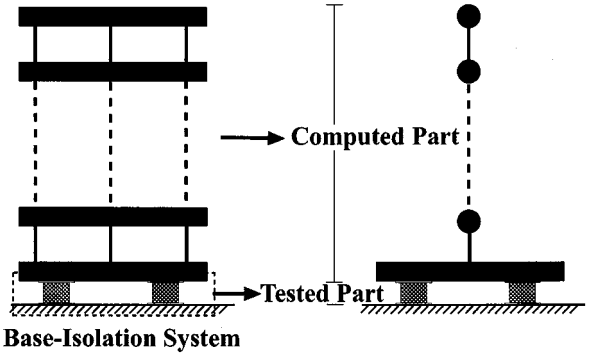

Figure 13. Multiple storey base-isolated building model considered and substructuring into tested and computed parts

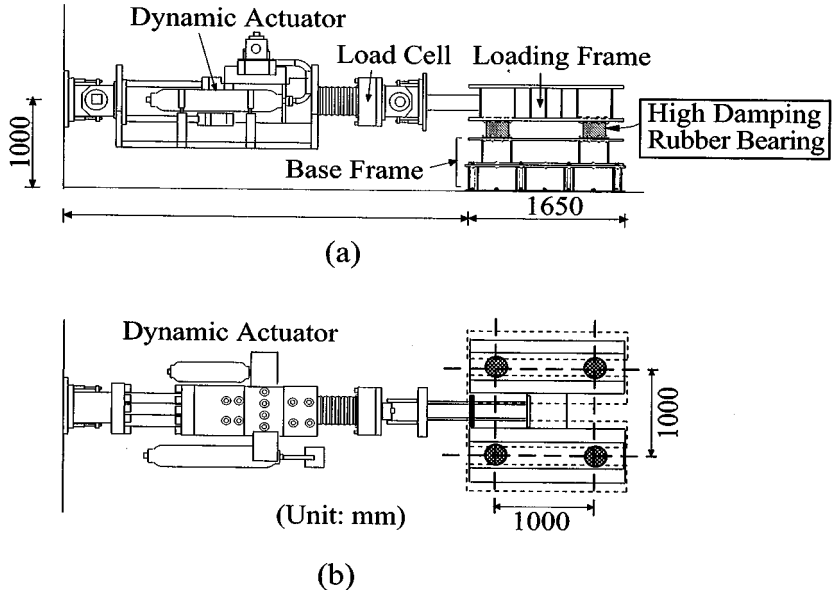

Figure 14. Test specimen and test set-up: (a) elevation; (b) plan

system (consisting of high damping rubber bearings) was taken as the tested part, the superstructure was modelled as a lumped-mass system and assigned as the computed part, and the equations of motion were formulated for the entire base-isolated building model. The test set-up, shown in Figure 14, features four identical rubber bearings securely fastened by high-tension bolts to the base steel frame at the bottom and to the loading steel frame at the top. The base steel frame is tied down to the strong floor, and the loading steel frame is attached by the dynamic actuator. The four rubber bearings are placed 1·0 m apart in the centre-to-centre length (Figure 14), and the actuator is attached so that it moves along the axis of symmetry of the base-isolation system. From a series of preliminary loading tests, it was found that the four rubber bearings would

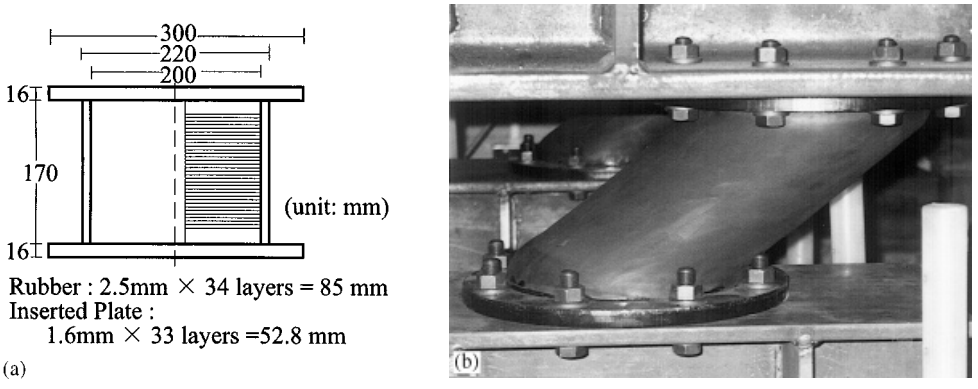

Figure 15. High damping rubber bearing: (a) geometrical properties; (b) a view for 200 per cent of shear strain

sustain almost the same displacement regardless of the level of deformation (meaning no torsion of the base-isolation system) and the displacement was nearly the same as the actuator's displacement, and therefore in the succeeding tests the actuator's displacement (measured by the actuator's LVDT) was taken as the displacement of the base-isolation system. The rubber bearings had the dimensions shown in Figure 15, with a total rubber thickness of 85 mm. Because rubber bearings popularly used in base-isolated buildings constructed in Japan are 150–200 mm in the total rubber thickness and 600–800 mm in the diameter, the tested rubber bearings are reduced models with a scale ratio of 1/3 to 1/4.

RESTORING FORCE CHARACTERISTICS OF THE BASE-ISOLATION SYSTEM

Before conducting real-time on-line tests, a series of dynamic loading tests subjected to sinusoidal displacements were carried out to examine how the restoring force characteristics of the base-isolation system would be affected by the imposed velocity and displacement. The displacement amplitude and frequency of sinusoidal motion were chosen as test variables. The displacement amplitudes selected were 30 mm ($\gamma = 36$ per cent), 42·5 mm ($\gamma = 50$ per cent), 85 mm ($\gamma = 100$ per cent), and 127·5 mm ($\gamma = 150$ per cent), with γ as the shear strain of the bearings. The frequencies chosen were 0·5, 1·0, 2·0, and 3·0 Hz. Tests with quasi-static loading (with the loading rate set at 0·01 mm/s) were also carried out for comparison. Figure 16(a) shows examples of hysteresis loops obtained, and Figures 16(b) and 16(c) show the obtained hysteretic characteristics in terms of the equivalent stiffness (k_{eq}) (the stiffness given as the slope of the line that connects the positive and negative extreme displacements) and the equivalent viscous damping ratio (h_{eq}). These figures clearly indicate that the hysteretic characteristics depend strongly on the frequency, loading cycle, and amplitude. This dependency demonstrates why on-line tests of base-isolated structures equipped with high damping rubber bearings have to be done on a real-time scale.

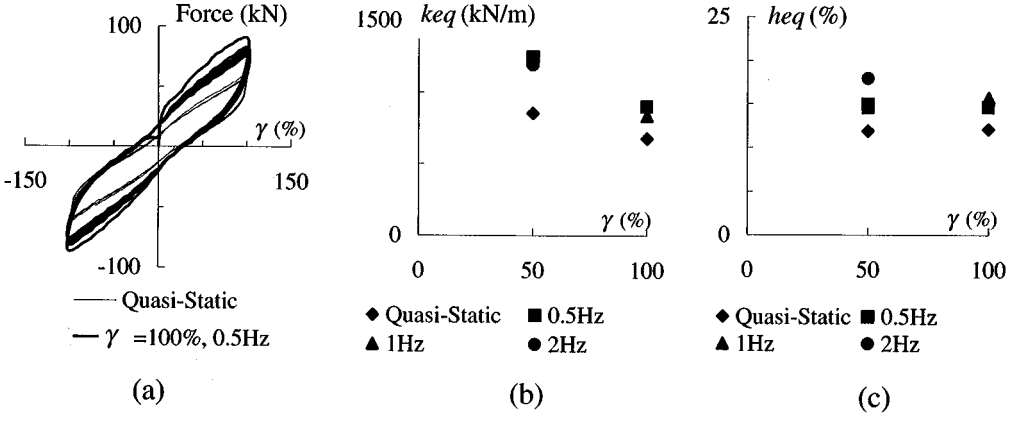

Figure 16. Results obtained from dynamic loading tests subjected to sinusoidal displacements: (a) restoring force relationship; (b) equivalent stiffness; (c) equivalent viscous damping ratio

VALIDATION OF EXTRAPOLATION, INTERPOLATION, AND DELAY COMPENSATION PROCEDUERES

To examine the effectiveness of the extrapolation, interpolation, and delay compensation procedures devised in the proposed system, a series of real-time on-line tests were carried out for an SDOF structure, in which a rigid mass was assumed on top of the base-isolation system. The central difference method was used to solve the equation of motion with an integration time interval (Δt) of 10 ms, which was the set value in the proposed system.

Delay compensation procedure

The tested SDOF structure was taken to be elastic and to have a viscous damping ratio of 2 per cent, and its free vibration responses subjected to an initial velocity were obtained from the real-time on-line test. In the test, the base-isolation system was actually loaded in accordance with the proposed on-line test procedure, with one exception: for the restoring force needed to solve the equations of motion with the time interval of Δt ($=10$ ms), the product of the computed target displacement and the assumed elastic stiffness of the SDOF structure was used instead of the measured force. This treatment was adopted to eliminate uncertainties related to the restoring force characteristics of the tested base-isolation system (which never behaves linearly). To look into the effect of response frequencies on the delay compensation procedure, the test was repeated for various natural frequencies (from 0·5 to 3·0 Hz) assigned to the SDOF structure. Here, 3·0 Hz was taken as the target response frequency below which the proposed system should guarantee accurate responses. This value was chosen considering that the proposed system is intended to serve as a tool for simulation of earthquake responses of building structures, and that most of structures have elastic fundamental natural frequencies not larger than 3·0 Hz.

Figure 17(a) shows the history of measured displacements (a dotted line), together with the target displacement histories created by solving the equation of motion (a solid line), for the

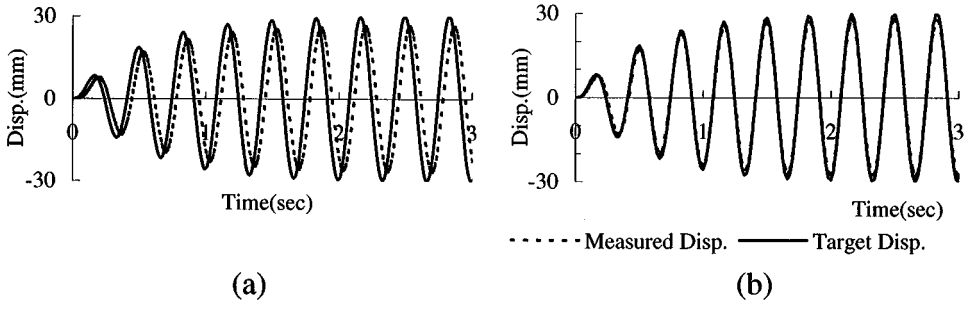

Figure 17. Effectiveness of actuator delay compensation procedure: (a) without delay compensation; (b) with delay compensation

natural frequency of 3·0 Hz with the delay compensation procedure not applied. This figure indicates that the actuator delay is approximately 30 ms throughout the response. Figure 17(b) shows the same histories but this time with the delay compensation procedure[13] applied, in which the initial delay time of 20 ms was adopted. A slight delay (by 4 ms) is present for the first and second cycles, but the delay is nearly zero (at most 1 ms) for the succeeding cycles, which verifies that the delay compensation procedure is effective.

Effectiveness of extrapolation and interpolation procedures

When the equations of motion to be solved have many DOFs, the time required for acquiring the next target displacement, which is executed by 'Response Analysis Task' in the proposed system, becomes longer, and as a result the number of extrapolations increases. To examine how many cycles of extrapolation can be tolerated in the proposed system, a series of real-time on-line tests were carried out for the base-isolated building model treated as an SDOF structure. In these tests, the force measured by the actuator's load cell was used to carry out the true real-time on-line test. Because the time needed to solve the equation of motion for an SDOF structure is short (in fact only one cycle of extrapolation is needed in the proposed system), a dummy 'DO loop' was inserted into the program that executes 'Response Analysis Task' in order to intentionally delay the creation of the next target displacement and increase the number of extrapolations. Input motion was taken as sinusoidal accelerations with various amplitudes and frequencies, and the mass of the SDOF structure was adjusted to provide approximately the resonance condition for a given set of amplitudes and frequencies of the input accelerations. Figure 18(a) shows an example of the obtained responses, the one for 1·0 Hz of the input acceleration frequency and accordingly responding with 1·0 Hz. The solid line shows the displacement history when the number of extrapolations was one (the minimum number required in the system), and the dotted line is the displacement history when the number of extrapolations was nine (the maximum number permitted in the system). The two responses are nearly identical, indicating that, for a response with 1·0 Hz, repeating the extrapolation nine times still ensures accurate responses. Figures 18(b)–18(d) are other examples, this time for 3·0 Hz of the input acceleration frequency. Up to six cycles of extrapolation, the response was very accurate [Figure 18(b)], but when the number of extrapolations increases to seven, the force response diverged quickly, and the test was brought to a stop [Figures 18(c) and 18(d)]. A closer examination into the displacement signals

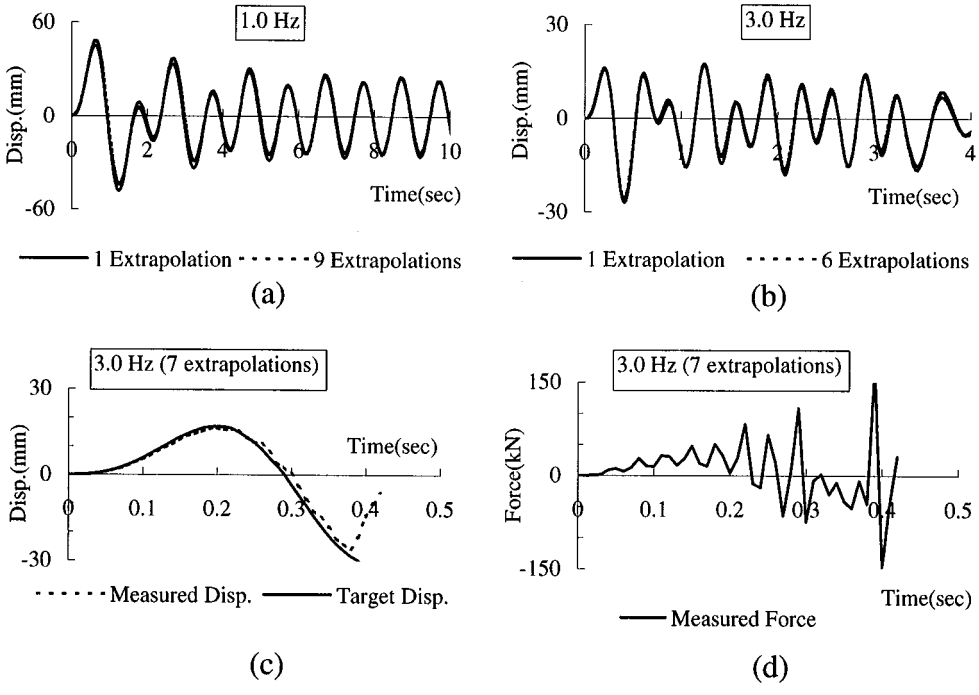

Figure 18. Effect of number of extrapolations on responses obtained from the real-time on-line test: (a) 1·0 Hz disp. response; (b) 3·0 Hz disp. response; (c) 3·0 Hz disp. response with seven cycles of extrapolation; (d) 3·0 Hz reactional force response with seven cycles of extrapolation

created for the interval of 1 ms (δt), target displacements provided after every 10 ms (Δt), and displacements measured after every 10 ms revealed that when the number is seven, the signals started fluctuating in the early response, and the fluctuation grew significantly afterwards. In this range a sudden change occurred in each integration time interval (10 ms) when the extrapolation procedure switched to the interpolation procedure, inevitably caused undesirable unloading and reloading during the interval, and made the reactional force versus displacement relationship very erroneous. The conclusion drawn from these tests is that the proposed system is able to ensure stable, accurate results up to the response of 3·0 Hz if the number of extrapolations remains not greater than six.

REAL-TIME ON-LINE TEST OF MULTI-STOREY BASE-ISOLATED BUILDING MODELS

Test involving large displacements and velocities

Real-time on-line tests were carried out for large earthquake motions to examine how the proposed system can trace earthquake responses involving large displacements and velocities. A five-storey base-isolated building model was considered, and the substructuring technique was

Table I. Structural and vibrational properties of the five-storey base-isolated building model

Storey	Mass (kg)	Storey stiffness (kN/m)	Mode	Natural circular frequency (rad/s)
Base-isolation	25 088	980	1st mode	2·51
1st storey	25 088	59 200	2nd mode	21·5
2nd storey	25 088	51 800	3rd mode	40·8
3rd storey	25 088	44 400	4th mode	57·4
4th storey	25 088	37 000	5th mode	71·1
5th storey	25 088	29 600	6th mode	85·2

employed (Figure 13). The superstructure was represented by an elastic five DOF structure with mass assumed to concentrate on each floor level and lateral stiffness of each storey provided by an elastic shear spring. The mass and stiffness properties of the model were specified according to the following assumptions: (1) the mass is equal for all storeys; (2) the storey stiffness distribution of the superstructure is linear, taking the stiffness at the top storey as half of the stiffness of the first storey; (3) the fundamental natural period of the superstructure is 0·5 s when its base is clamped; (4) viscous damping of the superstructure is initial stiffness proportional with the damping ratio of 2 per cent for the first mode of the superstructure and (5) the fundamental natural period of the whole structure including the base-isolation system is 2·5 s for the shear strain of the tested rubber bearings corresponding to 100 per cent, in which 980 kN/m of the secant stiffness is assigned for the base-isolation system in reference to the results obtained from forced displacement tests described earlier. The structural properties thus obtained are shown in Table I.

The periods of 0·5 s (for the fundamental natural period of the superstructure with the clamped base condition) and 2·5 s (for the fundamental natural period of the whole structure corresponding to the shear strain of rubber bearings equal to 100 per cent) are values typical of recent Japanese base-isolated buildings.[16] The following three ground motion histories were chosen for the input ground motion: El Centro-NS (1940), Hachinohe-EW (1968), and Point-B (1995). Hachinohe-EW is a history recorded in the 1968 Tokachioki Earthquake, which, because it contains a large component between 2·0 and 2·5 Hz in its response spectra and tends to cause large deformations in base-isolated buildings, has been used extensively in the design and analysis of Japanese base-isolated buildings.[17] Point-B is a synthesized ground motion[18] which simulates the ground motion in downtown Kobe during the 1995 Hyogoken–Nanbu (Kobe) Earthquake, and contains a large pulse-like component. In reference to the actuator's displacement and velocity capacities, the magnitude of the original acceleration histories was scaled to: 1·0 (meaning original) for El Centro-NS, 0·8 for Hachinohe-EW, and 0·5 for Point-B.

In these tests, the central difference method was used for direct integration, and the number of extrapolations remained one throughout loading. The displacement responses obtained from the tests are shown in Figure 19. In each of the response histories, six lines, each representing the displacement at a floor level (measured from the ground), are plotted together, but because the elastic superstructure responded nearly as a rigid mass, the six lines remain almost identical throughout the time. It is notable that Figure 19(b) (for Hachinohe-EW) indicates a few cycles of large displacements (reaching about 190 mm in the maximum), which is characteristic of the Hachinohe-EW response, and Figure 19(c) shows one cycle of a large displacement (also reaching about 190 mm in the maximum) as a result of a large pulse-like component included in Point-B.

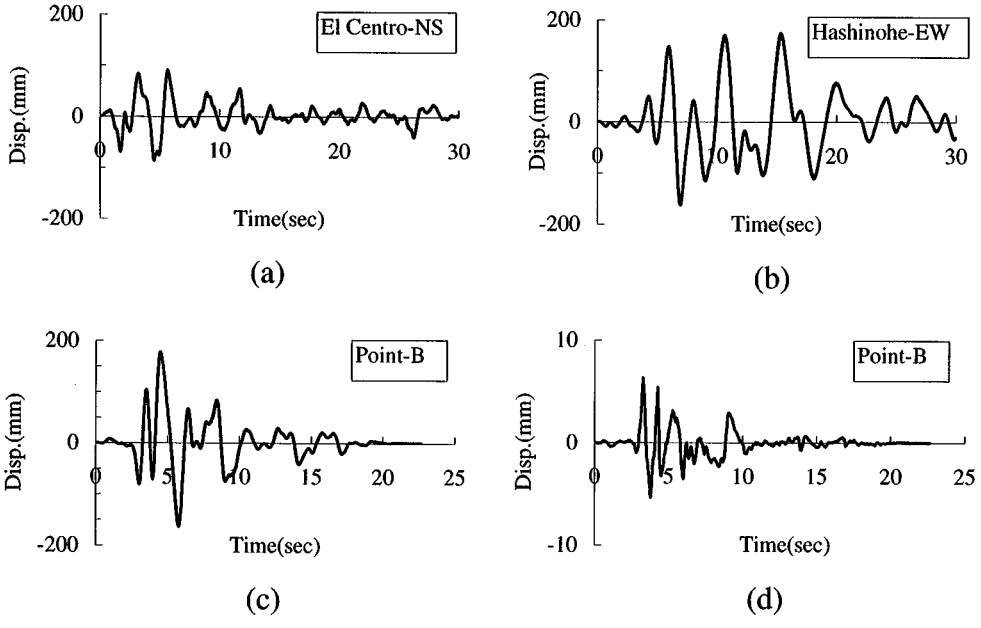

Figure 19. Displacement responses of the five-storey base-isolated building model subjected to large earthquake motions: (a) El-Centro-NS; (b) Hachinohe-EW; (c) Point-B; (d) Difference between computed (target) and measured displacements

Figure 19(d) shows a history of the difference between the target displacement and measured displacement obtained for every integration time interval (Δt). The difference is at most 5 mm and less than 3 per cent of the maximum displacement, demonstrating that accurate control is achieved in tracing large displacements. Figure 20(a) shows a numerically obtained displacement history for Point-B, together with the history obtained from the corresponding test. In the numerical analysis, the hysteresis of the base-isolation system was taken to be bilinear, with the initial stiffness, yield strength, and second stiffness adjusted in reference to the largest hysteresis loop obtained from the test. Correlation between the two responses is very good, but it is primarily because the numerical hysteresis was specified based on the experimental hysteresis. Figure 20(b) shows the velocity history for Point-B, also indicating good correlation between the experimental and numerical responses, with the maximum experimental velocity reaching 766 mm/s. Figure 20(b) verifies that velocity control was also successful in the test.

Tests with many DOFs

The number of extrapolations remained one for up to six DOF structures. The more DOFs are assigned in the equations of motion, the more extrapolations are required because of longer computation time. To investigate how many DOFs can be tested by the proposed system, 9- and 11-storey base-isolated building models, treated as 10 and 12 DOFs, respectively, were tested. The rules described for the five-storey base-isolated building model were adopted to specify the properties of the models, except for the fundamental natural period of the superstructure: 1·0 s

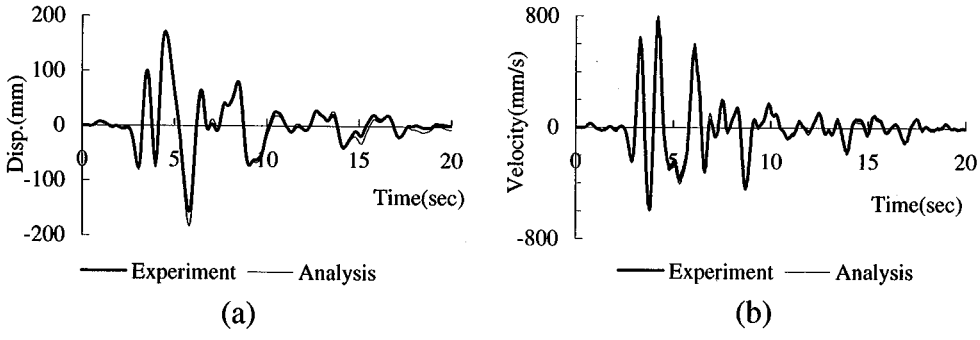

Figure 20. Comparison in response between test and numerical analysis (five-storey base-isolated building model subjected to Point-B earthquake motion: (a) displacement response of base-isolation system; (b) velocity response of base-isolation system

was chosen instead of 0·5 s because the period is longer for taller buildings. For each building model, tests were repeated for the three ground acceleration records, with the magnitude scaled to 0·2 of the respective originals, and sinusoidal ground accelerations with the frequencies of 0·5, 1·0, 2·0, and 3·0 Hz. In these tests, a direct integration algorithm that can ensure numerically stable responses in on-line tests applied to systems with many DOFs[7] was adopted instead of the conventionally used central difference method. Figure 21 shows examples of responses obtained. As shown in this figure, the earthquake responses have longer response periods ranging from 2·0 to 3·0 s (0·5 to 0·3 Hz) because of the flexibility of the base-isolation system, whereas the responses subjected to sinusoidal accelerations have dominant response frequencies equal to the respective input frequencies. The higher the response frequency is, the more difficult is the accurate control using the extrapolation and interpolation procedures, and for this reason sinusoidal ground accelerations were also chosen in the tests.

For the nine-storey model, all tests, including those with ground motion records and sinusoidal accelerations up to 3 Hz, were carried out successfully, as shown in Figures 21(a) and 21(b). In the meantime, the number of extrapolations needed for solving the equations of motion was three in these tests. For the 11-storey model, tests with ground motion records and sinusoidal accelerations up to 2·0 Hz were also completed successfully, as shown in Figures 21(c)–21(f), but the test with the sinusoidal acceleration of 3·0 Hz failed at 3·2 s [Figure 21(g)]. According to the corresponding reactional force history shown in Figure 21(h), the force starts fluctuating at about 1·0 s, and the fluctuation grows gradually between 1·0 and 1·5 s and is precipitated afterwards. This divergent behaviour is similar to what was observed in the test with the SDOF structure subjected to sinusoidal accelerations with 3·0 Hz [see Figures 18(c) and 18(d)], but a difference does exist in the number of extrapolations between the two tests; it was four in the 12 DOF test, while it was seven in the SDOF test. This suggests that the limitation of the proposed system was controlled not only by the number of extrapolations and response frequencies but also by the number of DOFs to be solved. A strong suspect is the behaviour characteristic of on-line tests when applied to structures with many DOFs, in which if reactional forces contain errors the highest mode vibration tends to grow erroneously.[15,19–21]

The conclusion drawn from these tests is that the proposed system is capable of performing the real-time on-line test with reasonable accuracy for up to 10 DOF structures with a range of

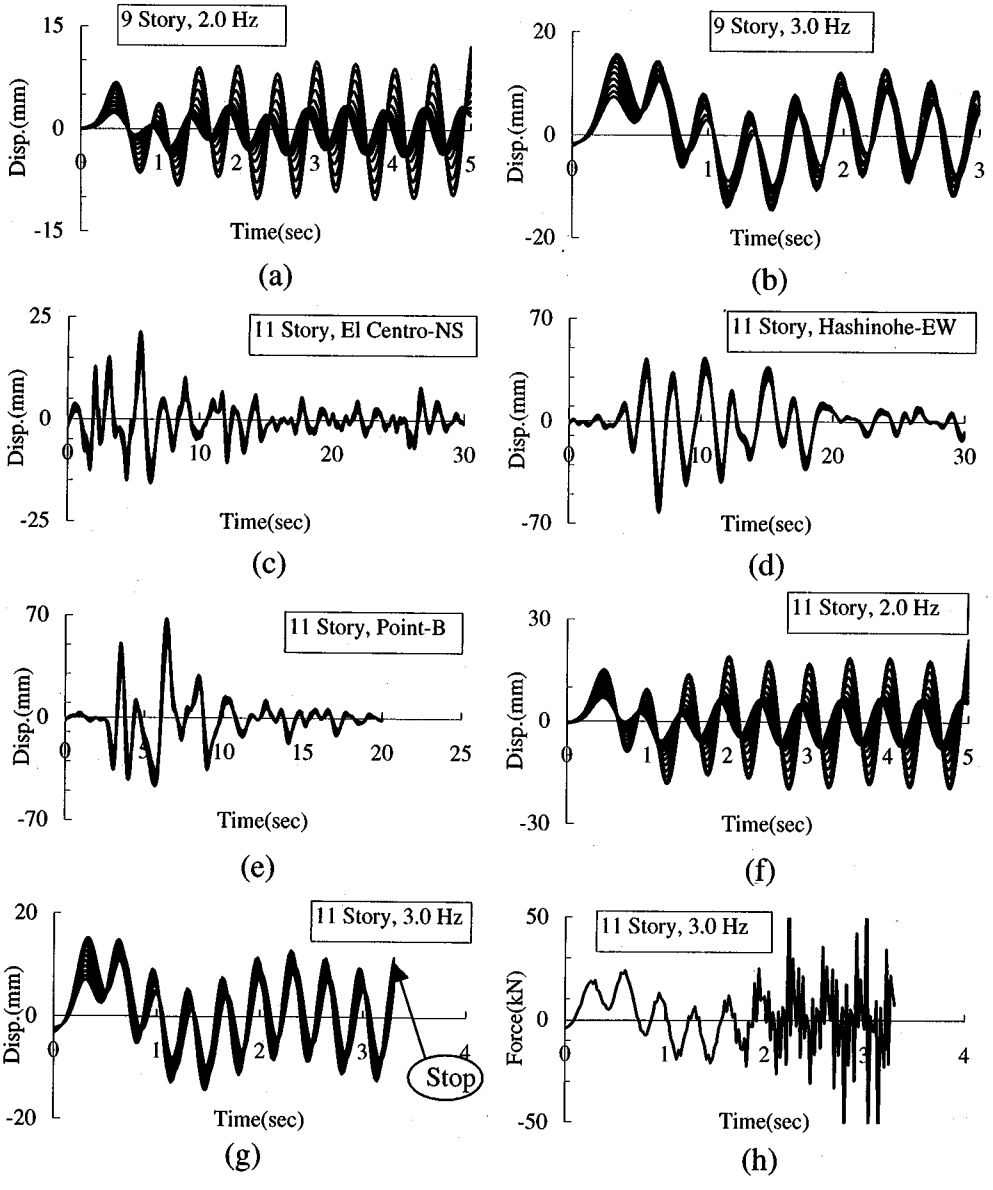

Figure 21. Displacement responses obtained for multi-storey base-isolated building models: (a) 9-storey model with 2·0 Hz motion; (b) 9-storey model with 3·0 Hz motion; (c) 11-storey model with El Centro-NS; (d) 11-storey model with Hachinohe-EW; (e) 11-storey model with Point-B; (f) 11-storey model with 2·0 Hz motion; (g) 11-storey model with 3·0 Hz motion (divergent response); (h) reactional force response of 11-storey model with 3·0 Hz motion (divergent response)

response frequency not greater than 3·0 Hz, or 12 DOF structures with a range of response frequency not greater than 2·0 Hz, beyond which erroneous reactional force responses impede sound application.

Tests for structures involving complex hysteresis

In the previous section, the time required for solving the equations of motion (and therefore the number of extrapolations) was enlarged by the increase in the number of DOFs. Another type of application that also requires a longer time for the solution of the equations of motion is described below. In the tests described up to this section, the superstructure was taken to behave only linearly, but under large earthquake motions the superstructure may behave beyond the elastic range even if it is base-isolated. With this condition, the number of DOFs remains the same between the elastic and inelastic superstructures, but a longer time is required in the inelastic structure in order to create the next target displacement, because; (1) more variables are needed for the solution program, requiring a larger program and (2) reactional forces of the superstructure have to be obtained in reference to the hysteresis models incorporated into the program, which makes the computation longer.

To emulate such a situation, the five-storey building model presented earlier was considered, which required one cycle of extrapolation if the superstructure was assumed to behave elastically. This time, each storey of the superstructure was assumed to behave in a bilinear manner. The storey yield force was adjusted to 40 per cent of the maximum storey shear force obtained for the model with the elastic superstructure, and the second stiffness was equal to 10 per cent of the initial stiffness. The Hachinohe-EW was used for input motion, with the magnitude scaled to 0·2 of the original. The obtained responses are shown as the solid line in Figure 22(a). The number of extrapolations was found still to be one for this test. Next, the number of bilinear hysteresis models was increased successively in the following manner. For each storey, the bilinear relationship was divided equally into n bilinear relationships, each of which had an initial stiffness and a yield force equal to $1/n$ of the original elastic stiffness and yield force, respectively, and these divided relationships were connected in parallel as shown in Figure 23. With this treatment, the sum of the n divided bilinear relationships becomes identical to the original bilinear relationship, so that the responses would remain identical regardless of the number of n. The real-time on-line test was repeated with the number of n increased successively from 2 to 30. Here, with the increase in n, the time required for solving the equations of motion became large, and the number of extrapolations increased accordingly. The dotted line in Figure 22(a) shows the responses obtained from the model having 30 divided bilinear relationships [meaning a total of 150 (30 per

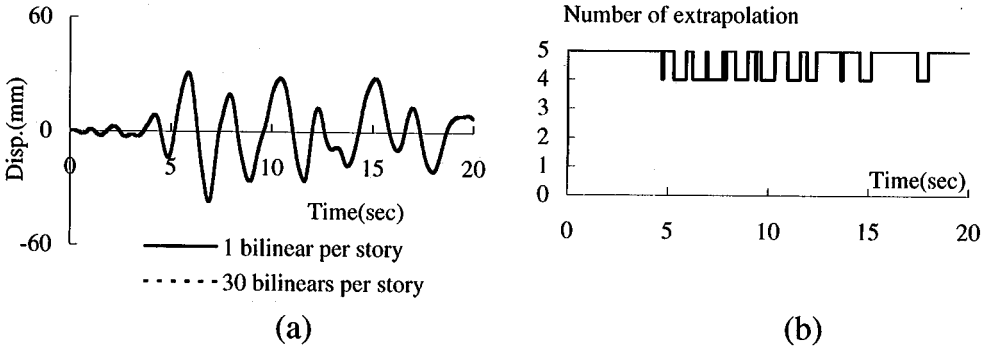

Figure 22. Responses obtained for the five-storey base-isolated building model having inelastic superstructure: (a) displacement response of base-isolation system; (b) number of extrapolations

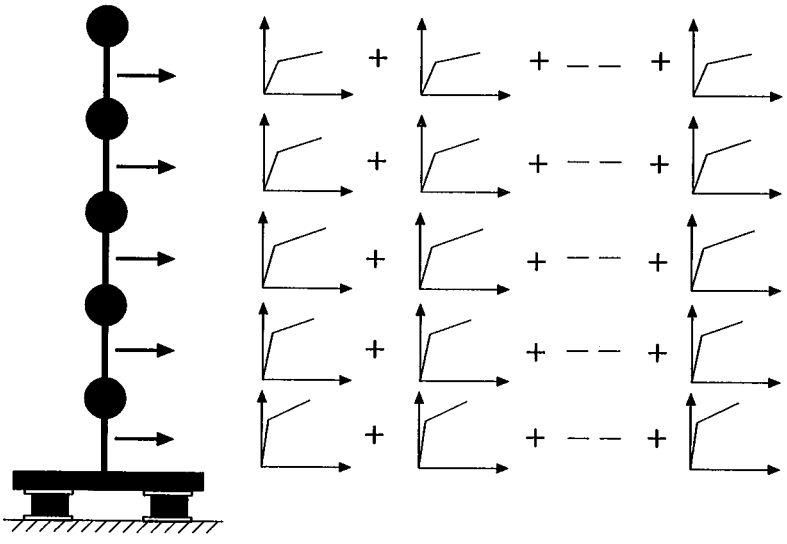

Figure 23. Inelastic characteristics assigned for the superstructure of the five-storey base-isolated building model

storey times five storeys) divided bilinear relationships embedded in the solution program]. The number of extrapolations required was either four or five in this test, as shown in the number of extrapolations history in Figure 22(b). The solid and dotted lines of Figure 22(a) are almost identical, which verifies that the response is simulated accurately even if the program contains 150 bilinear relationships. This test was achieved primarily thanks to the separation of 'Response Analysis Task' and 'Signal Generation Task', as specifically devised in the proposed system, and demonstrates the power of the system for conducting real-time on-line tests of complex structures.

APPRAISAL OF PROPOSED SYSTEM IN COMPARISON WITH SHAKING TABLE SYSTEMS

It is worth noting the advantages and drawbacks of the real-time online test developed in this study relative to the shaking-table test, which is known to be the most direct method for simulating earthquake responses of structures. For example, in the five-storey base-isolated building model tested in this study, the mass per story was assigned as 25 088 kg, which is equivalent to a total weight of about 1500 kN. Since the mass was taken into account in the computer, no real weight was needed in the test — one of the largest assets of the on-line test. If the same building model is to be tested on a shaking table, an actual weight equal to 1500 kN is required. In most shaking tables of medium size, say, tables having dimensions of few meters by few meters, the weight capacity is at most about several hundred kN,[22] which is far smaller than the weight needed for the test. As this simple example verifies, the real-time on-line test has a significant advantage over the shaking-table test in terms of the size of the structures that can be tested. The substructuring technique was employed in the tests presented in the study, and

therefore a physical model representing the superstructure need not be fabricated, whereas in the shaking-table test, a physical model must be installed on the table. This is one of the significant advantages of the on-line test in general, and the real-time on-line test can also utilize this benefit.

Because base-isolated building structures were chosen in the tests, extracting the base-isolation system for the real test and handling the superstructure numerically was justified, because the restoring force characteristics of the base-isolation system are complex and depend strongly on the displacement and velocity, whereas the superstructure behaves more or less linear elastically. If complex inelastic behaviour spreads through the structure concerned, however, one can no longer designate any specific portion as the tested part. If complex inelastic behaviour is expected in, say, 20 locations and yet one is forced to try an on-line test, many substructured test pieces need be prepared, many actuators are required for loading the individual test pieces, and furthermore proper boundary conditions have to be assigned for each test piece to ensure overall compatibility. In such a case, the logical choice is naturally a shaking-table test.

In the proposed system, response frequencies beyond 3·0 Hz are not guaranteed, primarily because of limitations of the extrapolation and interpolation procedures. There is no such limitation in the shaking-table test, meaning that the shaking-table test is more reliable for simulating the earthquake response of very stiff structures.

Another appealing method for realizing the real-time on-line test was suggested by Thewalt and Mahin[23] in the mid-1980s and has been explored lately in greater detail.[24] In this method, the actuator is force-controlled, and the force time history is provided *a priori* as the product of the structural mass and the ground acceleration; therefore the equations of motion need not be solved at all. The method, however, requires a real structural mass in order to obtain the true reactional force (to be detected by the load cell for feedback control). This implies that if the five-storey base-isolated building model tested in this study is to be tested by that method, a weight equal to 1500 kN must be attached to the base-isolation system, which may not be an easy task in real implementation. There is still much room for further advancement of the real-time on-line test, as evidenced also in this study (in which the proposed system failed in simulating the 3·0 Hz response of a 12 DOF structure), and the writers are not fully confident that the proposed system is superior in all aspects to the one being developed in References 23 and 24. More careful examination of the relative merits between the two systems is needed.

CONCLUSION

This paper presented a test system for conducting the on-line test in a real time and a series of real-time on-line tests to verify the effectiveness of the system. Summary and conclusions are as follows:

(1) Main features of the system include: (1) use of a Digital Signal Processor (DSP) now readily available, (2) adoption of the C language to ensure easy programming and (3) separation of response analysis and displacement signal generation so that the system could be used to test complex structures. A computer for real-time on-line test was devised to achieve these features. The computer has two major tasks: creating the target displacement after every 10 ms (Δt) by solving the equations of motion, and creating displacement signals successively with an interval of 1 ms (δt). The two tasks were programmed as independent procedures with minimal exchange of information between them, thus ensuring flexible programming

for the solution of equations of motion. Separation of the two tasks also enables us to test complex structures in which a longer time is required to solve the equations of motion.

(2) To create displacement signals, the extrapolation and interpolation procedures were developed. The accuracy of the procedures in predicting displacement signals was examined through analytical formulation, and the effectiveness of the third-order polynomial in terms of accurate displacement and velocity prediction was verified. Base-isolated building models were chosen for the real-time on-line test, and the effectiveness of the extrapolation and interpolation procedures was demonstrated through a series of real-time on-line tests applied to the models treated as SDOF structures.

(3) A five-storey base-isolated building model (treated as a six DOF structure) was tested for various ground motions, and it was verified that the system is able to successfully simulate earthquake responses involving large displacements (up to ± 200 mm) and large velocities (up to ± 700 mm/s).

(4) The number of DOFs that can be handled in the proposed system was investigated, and it was found that the system is capable of performing the test with reasonable accuracy on up to 10 DOF structures with a range of response frequency not greater than 3·0 Hz, or on 12 DOF structures with a range of response frequency not greater than 2·0 Hz, beyond which the system failed in simulating the response.

(5) A real-time on-line test in which the superstructure behaved inelastically was conducted, and responses of a five-storey base-isolated building model into which 150 bilinear relationships were incorporated were obtained successfully.

ACKNOWLEDGEMENTS

The writers are grateful to Prof. T. Nonaka of Kyoto Univ. for his encouragement in carrying out this study. Part of this study was supported by the Kajima Foundation to which the writers express their appreciation. Appreciation is also extended to the following individuals: Mr. S. Tanaka of Micro Signal Co. and Messrs. T. Konno and H. Koike of Hitachi Co. for their continuous support when developing the test system described in this paper, and Messrs. T. Kawai and Y. Miyauchi of Toyo Rubber Co. for their assistance in the fabrication of the base-isolation system used in the test.

REFERENCES

1. K. Takanashi *et al*., 'Nonlinear earthquake response analysis of structures by a computer actuator online system (Part 1, details of the system)', *Trans. Arch. Inst. Japan* **229**, 77–83 (1975) (in Japanese).
2. T. Okada and M. Seki, 'Nonlinear earthquake response of reinforced concrete building frames by computer-actuator on-line system (Part 1, objective and methodology)', *Trans. Arch. Inst. Japan* **275**, 25–31 (1979) (in Japanese).
3. S. A. Mahin and P. B. Shing, 'On-line method of seismic testing', *J. Struct. Engng. ASCE* **111**(7), 1482–1503 (1985).
4. K. Takanashi and M. Nakashima, 'Japanese activities on online testing', *J. Engng. Mech. ASCE* **113**(7), 1014–1032 (1987).
5. S. A. Mahin, *et al*., 'On-line test method — current status and future directions', *J. Struct. Engng. ASCE* **115**(8), 2113–2128 (1989).
6. P. B. Shing, M. Nakashima and O. S. Bursi, 'Application of pseudodynamic test method to structural research', *Earthquake Spectra* **12**(1), 29–56 (1996).
7. M. Nakashima, *et al*., 'Integration techniques for substructure online test', *Proc. 4th U.S. National Conf. on Earthquake Eng*., Palm Springs, CA, II, 1990, pp. 515–524.
8. P. B. Shing, M. T. Vannan and E. Carter, 'Implicit time integration for online tests', *Earthquake Engng. Struct. Dyn.* **20**, 551–576 (1991).
9. M. Nakashima, H. Kato and E. Takaoka, 'Development of real-time pseudo dynamic testing', *Earthquake Engng. Struct. Dyn.* **21**, 79–92 (1992).

10. T. Horiuchi *et al*., 'Development of real-time hybrid experimental system with actuator delay compensation', *Proc. 9th Japan Symp. on Earthquake Engng*. 1994, pp. 1531–1536 (in Japanese).
11. K. Umekita, M. Kametani and N. Miyake, 'Development of super real-time controller which can perform analysis along with measurement/control in real time', *Proc. 5th Robot Symp*., Robotics Society of Japan, 1995, pp. 55–58 (in Japanese).
12. T. Horiuchi *et al*., 'Development of a real-time hybrid experimental system with actuator delay compensation', *Proc. 11th World Conf. on Earthquake Engng*., *Paper #660*, 1996.
13. T. Horiuchi *et al*., 'Development of a real-time hybrid experimental system with actuator delay compensation (Part 1: compensation method and application to experiments of single-degree-of-freedom systems)', *Trans. Japan Soc. Mech. Engng*. **61**(584), 64–72 (1995) (in Japanese).
14. T. Horiuchi *et al*., 'Development of a real-time hybrid experimental system with actuator delay compensation (Part 2: application to a multiple-degree-of-freedom system)', *Trans. Japan Soc. Mech. Engng*. **62**(599), 47–54 (1996) (in Japanese).
15. M. Nakashima and H. Kato, 'Part 3, Experimental error growth of online testing (stability and accuracy behavior of online response)', *J. Struct. Construct. Engng. Arch. Inst. Japan* **386**, 36–48 (1988).
16. M. Nakashima, 'Deformation behavior of base-isolated buildings in near-fault earthquakes', *Proc. IABSE Symp. on Long-Span and High-Rise Structures*, Kobe, 1998, pp. 655–660.
17. 'Building letters', The Building Center of Japan, Tokyo, 1996, pp. 348–359 (in Japanese).
18. Y. Hayashi and H. Kawase, 'Strong motion evaluation in Chuo Ward, Kobe, during the Hyogoken-Nanbu Earthquake of 1995', *J. Struct. Construct. Engng. Arch. Inst. Japan* **481**, 37–46 (1996) (in Japanese).
19. P. B. Shing and S. A. Mahin, 'Cumulative experimental errors in online test', *Earthquake Engng. Struct. Dyn.* **15**, 409–424 (1987).
20. P.B. Shing and S. A. Mahin, 'Experimental error effects in pseudodynamic testing', *J. Engng. Mech. ASCE* **116**(4), 805–821 (1990).
21. M. Nakashima and H. Kato, 'Part 4, Control of experimental error growth of online testing (stability and accuracy behavior of online response)', *J. Struct. Construct. Engng. Arch. Inst. Japan* **401**, 129–138 (1989).
22. K. Kamimura, Y. Aoki and M. Nakashima, 'CIB register of world large scale test facilities for building research', *CIB Report*, 1984.
23. C. R. Thewalt and S. A. Mahin, 'Hybrid solution techniques for generalized pseudodynamic testing', *Report UBC/EERC-87/09*, Earthquake Engineering Research Center, University of California, 1987.
24. J. Murcek *et al*., 'Effective force testing: a method of seismic simulation for structural testing', *J. Struct. Engng. ASCE* (accepted for publication).

